BUTTERWORTH HEINEMANN

Cooling of stacks of plates shielded by porous screens

A. Bejan
Department of Mechanical Engineering and Materials Science, Duke University, Durham, NC, USA

S. J. Kim
Thermal Engineering Center, IBM SSD, Tucson, AZ, USA

Al. M. Morega
Department of Mechanical Engineering and Materials Science, Duke University, Durham, NC, USA

S. W. Lee
Mechanical Technology Department, IBM NS, Research Triangle Park, NC, USA

This paper addresses the question of how to cool a stack of parallel, heat-generating boards when the flow is impeded by electromagnetic screens placed upstream and downstream of the stack. Four separate designs are considered: (1) forced convection cooling of a stack with board-to-board spacing selected to minimize the stack-coolant thermal resistance; (2) forced convection cooling of stack with fixed board-to-board spacing; (3) natural convection cooling of a vertical stack with spacing selected to minimize the overall thermal resistance; and (4) natural convection cooling of a vertical stack with fixed spacing. The optimal spacings in designs (1) and (3) are determined by intersecting the known asymptotic solutions for stacks with small spacings and stacks with large spacings. The results of parts (1) and (2) are extended to applications where the stack is cooled by immersion in a free stream. We show that the effect of the screen is controlled by a single dimensionless group, which is identified for each class of designs; namely, forced versus natural convection, and high- versus low-screen Reynolds number. Engineering results are reported for the design of screens made of wire meshes, or perforated plate with square (sharp) edges.

Keywords: electronic cooling; forced convection; natural convection

Introduction

Microelectronics packaging is subject to several conflicting requirements, such as electromagnetic compatibility, acoustic limits, and adequate cooling. Electronic systems and components are often enclosed completely inside conducting cases to minimize radio frequency interference or electromagnetic interference, or for protection against airborne particles (Steinberg 1980). These enclosures have the added benefit that they reduce the sound pressure level associated with acoustic noise generation.

There are numerous applications where the thermal design rules out use of a complete enclosure around the electronic package. Openings must be provided in the enclosure because the cooling requirement of an enclosed packages is greater and the need to ventilate the electronic components becomes critical. This conflict between the need to enclose and the need to cool poses a significant design challenge as the power density of electronics is increased.

A design rule for the enclosures of commercial products calls for apertures whose linear dimensions should not exceed 1/20th of the source wavelength (Ott, 1988). Furthermore, when apertures of equal size are placed close to one another, the reduction in shielding effectiveness is approximately proportional to the square root of the number of apertures. From a cooling standpoint, however, it is advantageous to increase the number and size of the apertures to reduce the enclosure resistance to air flow. The questions that follow are: How many apertures should be used?; and What should be the aperture size so that the overall design meets the electromagnetic compatibility, acoustic, and thermal specifications?

The importance of the optimal selection of openings for air cooling has been recognized in the design of stacks of parallel printed circuit boards. The stack with vertical boards cooled by natural convection has been optimized by Anand et al. (1990, 1992), Bar-Cohen and Rohsenow (1984), Elenbaas (1942), Kim et al. (1991) and Levy (1971). The forced convection cooling of stacks of parallel boards was optimized by Bejan (1993), Bejan and Sciubba (1992), Hirata et al. (1970), Matsushima et al. (1992) and Nakayama et al. (1988). For both cooling modes, the board-to-board spacing was selected so that the total heat transfer from the stack (or the heat generation rate per unit stack volume) is maximized. In all these studies, the stacks were immersed in the coolant; i.e., they were not placed inside enclosures.

Address reprint requests to Professor Bejan at the Department of Mechanical Engineering and Materials Science, Duke University, Box 90300, Durham, NC 27708-0300, USA.

Received 8 March 1994; accepted 25 August 1994.

Int. J. Heat and Fluid Flow 16: 16–24, 1995
© 1995 by Elsevier Science Inc.
655 Avenue of the Americas, New York, NY 10010

0142-727X/95/$10.00
SSDI 0142-727X(94)00011-Z

The objective of the present work is to optimize the thermal performance of stacks of parallel boards that are surrounded by permeable (perforated) screens. The study is structured as a sequence of four distinct problems, according to the cooling mode (forced convection *vs.* natural convection), and whether the board-to-board spacing is fixed or constitutes a degree of freedom in the design. In every case, we seek to establish the relation between the characteristics of the perforated screens (e.g., porosity) and the overall thermal conductance between the stack and the coolant.

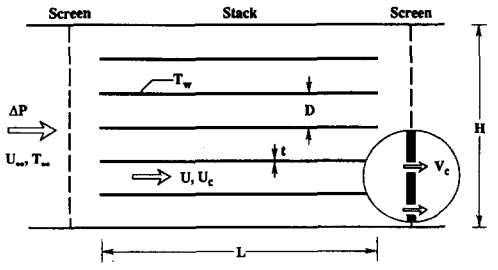

Figure 1 Forced convection cooling of a stack of parallel plates with inlet and outlet screens

2. Forced convection: large screen Reynolds numbers

Consider the $L \times H$ stack of heat-generating parallel plates (e.g., printed circuit boards) shown in Figure 1. It is assumed that the stack dimension perpendicular to the figure is sufficiently greater than the plate-to-plate spacing D so that the flow through each channel is two-dimensional (2-D). Two electromagnetic screens (e.g., perforated plates) are placed immediately upstream and downstream of the stack. The coolant (e.g., air) is forced to flow through the entire assembly by the pressure difference ΔP, which is fixed. The flow through the spaces between the parallel plates is laminar.

2.1 Optimal plate-to-plate spacing

The first problem we address is how to select the number of plates in the stack (or the spacing D) so that the overall thermal conductance between the stack to the coolant is maximum. The method of solution will be the same as in Bejan (1993), in which the stack without inlet and outlet screens was optimized by identifying the two asymptotic regimes (small D, large D) and intersecting the two asymptotes. It was shown that the optimal spacing determined in this manner agrees within 20 percent with considerably more accurate optimization results based on an entrance-region analysis of each channel (Bejan and Sciubba 1992), or on numerical simulations of the entire package (Morega, and Bejan 1994). The reliability and accuracy of the method are discussed further in Section 6.

To be able to highlight analytically the effect of the inlet and outlet screens, we treat the plate thickness t as negligible relative to the spacing D. Accordingly, we write that the number of plates installed in the stack is as follows:

$$n = H/D \tag{1}$$

where n is assumed considerably greater than 1. It has been shown that the optimal spacing derived in this manner for the stack without screens is correct even when the $t \ll D$ assumption is not valid (Mereu et al. 1993).

We begin with the $D \to 0$ asymptotic regime, where the flow through each D channel is of the Hagen–Poiseuille type. The pressure drop across the stack, from the plane situated behind the inlet screen to the plane in front of the outlet screen, is as follows:

$$\Delta P_s = 12\,\mu\, LU/D^2 \tag{2}$$

where U is the longitudinal velocity averaged over the D spacing. The total pressure difference maintained across the entire assembly is as follows (Ellison, 1984):

$$\Delta P = \Delta P_s + 2\,K_c\,(1/2)\rho\, V_c^2 \tag{3}$$

Notation

c_P	specific heat at constant pressure, J/kg K
d	wire diameter, m
D	plate-to-plate spacing, m
D_{opt}	optimal spacing, m
g	gravitational acceleration, m/s^2
k	stack thickness in Figure 1; stack height in Figure 6, m
R	fluid thermal conductivity W/mk
K_c	screen pressure loss coefficient
L	stack length in Fig. 1; stack thickness in Fig. 6, m
$\dot{m}'$	mass flow rate, kg/s·m
n	number of plates
p	parameter, Equation 14
p_*	parameter, Equation 34
Pr	Prandtl number
q'	total heat transfer rate, W/m
q'_1	heat transfer through one side, W/m
Ra_H	Rayleigh number, Equation 33
Re_d	screen Reynolds number, $U_\infty d/\nu$
Re_L	Reynolds number, $U_\infty L/\nu$
t	plate thickness, m
T_c	core temperature, K
T_w	plate temperature, K
T_∞	ambient temperature, K
U	mean velocity, m/s
U_c	core velocity, m/s
U_∞	free-stream velocity, m/s
V_c	mean velocity through orifice, m/s
x	screen parameter, Equation 14
x_*	*screen parameter, Equation* 34
y	screen parameter, Equation 23
y_*	screen parameter, Equation 43

Greek symbols

α	thermal diffusivity, m^2/s
β	coefficient of thermal expansion, K^{-1}
δ	dimensionless spacing, Equation 13
δ_*	dimensionless spacing, Equation 34
ΔP	total pressure drop, N/m^2
ΔP_s	stack pressure drop, N/m^2
θ	dimensionless core temperature, Equation 33
λ	screen pressure loss coefficient
μ	viscosity, kg/s·m
ν	kinematic viscosity, m^2/s
Π	pressure drop number, Equation 13
ρ	density, kg/m^3
$\bar{\tau}$	average wall shear stress, N/m^2
φ	screen porosity

because of the pressure drops across the screens (the factor 2 preceding K_c accounts for the number of screens). Much experimental data on the contraction pressure loss coefficient K_c are available already (Bernardi et al. 1976; Blevins 1992; Idelchik et al. 1986). The experiments showed that when the Reynolds number based on screen orifice size is of order 500 or greater; K_c does not depend upon the Reynolds number and is only a function of the screen porosity φ, which is defined as the total cross-sectional area of all the orifices, divided by the frontal area of the screen. For example, Idelchik et al.'s K_c correlation for a screen made of wire with square cross section, or plate with perforations with square (sharp) edges is as follows:

$$K_c = (1/\varphi)^2[0.707(1-\varphi)^{1/2} + 1 - \varphi]^2 \tag{4}$$

The K_c values calculated with Equation 4 agree within 10 percent with the K_c values tabulated for the same geometry by Blevins (1992).

In electronic equipment cooling applications, the inlet air velocity is typically of order 1.5 m/s; whereas, the screen perforations (e.g., punched holes) have diameters of order 0.5 cm. This means that Reynolds number based on hole diameter is of order 500, and we can regard K_c as a function of only φ. Indeed, one important unknown in the design is the screen porosity φ or, if the perforation size is given, the number of perforations per unit area.

We also assume that the screen orifices (e.g., holes, slits) are sufficiently numerous and identical in size and are distributed uniformly over the screen so that they do not interfere with (i.e., do not cause flow maldistributions in) the grid of spacing D formed by the stack. The longitudinal velocity averaged over the cross-sectional area of one orifice (V_c, see Figure 1, detail) is related to the stack mean velocity U by the following mass conservation relation:

$$V_c = U/\varphi \tag{5}$$

To summarize the behavior of the flow in the small D regime, we combine Equations 2, 3, and 5 into an implicit relation between the mean velocity through the stack U and the imposed pressure difference ΔP

$$\Delta P = 12\mu(LU/D^2) + (K_c/\varphi^2)\rho U^2 \tag{6}$$

In the same regime of sufficiently small spacings D, the outlet temperature of the coolant is equal to the temperature of the plates in the stack T_w. The total heat transfer from the stack to the coolant is $q' = \dot{m}' c_p (T_w - T_\infty)$, where $\dot{m}' = n\rho UD$ and $n = H/D$:

$$q'_{\text{small } D} = \rho U H c_p (T_w - T_\infty) \tag{7}$$

At the end of this section, Equations 6 and 7 are combined numerically to eliminate U and express the overall thermal conductance $q'/(T_w - T_\infty)$ as a function of the imposed ΔP and the design variable D.

When the plate-to-plate spacing is large enough that each plate is lined by distinct boundary layers, the pressure drop across the stack is as follows:

$$\Delta P_s = 2L\bar{\tau}/D \tag{8}$$

where $\bar{\tau}$ is the wall shear stress averaged over the plate length (e.g., Incropera and DeWitt 1990),

$$\bar{\tau} = 0.664\rho U_c^2 (U_c L/\nu)^{-1/2} \tag{9}$$

The assumption that D is sufficiently large means that the order of magnitude of D is greater than the boundary-layer thickness scale, and U_c is the longitudinal velocity in the core of the D channel; i.e., outside the two boundary layers that sandwich the core. The pressure drop caused by the two screens is the same as the second term in Equation 3; in other words, Equation 3 applies in the large D regime as well. By combining Equations 3, 8, and 9, we obtain an implicit relation between the stack core velocity and the overall pressure difference

$$\Delta P = 1.328(L/D)\rho U_c^{3/2}(\nu/L)^{1/2} + (K_c/\varphi^2)\rho U_c^2 \tag{10}$$

The core velocity U_c is needed to evaluate the heat transfer through one boundary layer (e.g., Bejan 1993); namely, $q'_1 = 0.664\, k(T_w - T_\infty)\,\mathrm{Pr}^{1/3}\,(U_c L/\nu)^{1/2}$, and total heat transfer from the stack, $q' = 2nq'_1$ or

$$q'_{\text{large } D} = 1.328k(T_w - T_\infty)(H/D)\,\mathrm{Pr}^{1/3}\,(U_c L/\nu)^{1/2} \tag{11}$$

where k is the fluid thermal conductivity. To summarize the large D analysis, the core velocity U_c can be eliminated numerically between Equations 10 and 11 to relate the overall thermal conductance $q'/(T_w - T_\infty)$ to the variable spacing D and the fixed overall pressure difference ΔP.

The third and final step in this analysis is the observation that the optimal spacing D_{opt} that maximizes $q'(T_w - T_\infty)$ is approximately the same as the D value where the small D and large D asymptotes intersect. The geometric reasons for this observation are given in Bejan and Sciubba (1992). We locate the D intersection by using the right-hand sides of Equations 7 and 11 to write $q'_{\text{small } D} = q'_{\text{large } D}$, and the resulting relation is as follows:

$$UD_{\text{opt}}/\nu = 1.328\,\mathrm{Pr}^{-2/3}(U_c L/\nu)^{1/2} \tag{12}$$

In conclusion, the preceding analysis produced a system of three equations: namely, Equations 6, 10, and 12, all written for $D = D_{\text{opt}}$, to determine the three unknowns of the problem: D_{opt}, U, and U_c. This system can be solved numerically, by first introducing the following dimensionless notation:

$$\delta = (D_{\text{opt}}/L)\Pi^{1/4}, \qquad \Pi = \Delta P \cdot L^2/\mu\alpha \tag{13}$$

$$x = (K_c/\varphi^2)\mathrm{Pr}^{-5/3}, \qquad p = (UL/\alpha)\Pi^{-1/2} \tag{14}$$

If we use this notation, the problem reduces to solving the following system:

$$12p/\delta^2 + xp^2\,\mathrm{Pr}^{2/3} = 1 \tag{15}$$

$$0.332x\,\delta^4 p^4\,\mathrm{Pr}^{4/3} + 0.567\,\delta^2 p^3 = 1 \tag{16}$$

Equation 15 follows from Equation 6; whereas, Equation 16 results from eliminating U_c between Equations 10 and 12.

The general numerical solution is presented in Figure 2 as the optimal δ *versus* the x number: this accounts for the effect of screen porosity (through φ and K_c), the effect of screen geometry (through K_c: perforated *versus* woven screen, sharp *versus* rounded edges), and the effect of fluid type (through Pr). We see that when the screens are absent ($x = 0$) the optimal spacing parameter approaches $\delta = 2.73$. In the opposite limit ($x \gg 1$), the optimal spacing approaches $\delta = 1.32\ x^{1/4}$. It is worth noting that in both x limits, the $\delta(x)$ relation is independent of Pr: this feature is the result of including Pr in the definition of x, Equation 14. The Prandtl number has the peculiar effect that it shifts the minimum of the $\delta(x)$ curve; however, this is a minor effect in the Pr range 0.72–7. It was shown, based on a more accurate analysis in Bejan and Sciubba (1992), that the optimal spacing corresponds to a developing channel flow where the thermal boundary layers just meet at the exit; i.e., where L is the thermal entrance length.

Along the top of Figures 2 and 3, we plotted the porosity that corresponds to the abscissa parameter x when the coolant is air (Pr = 0.72), and the screen is a plate with sharp-edge perforations. For the function $K_c(\varphi)$ we used the values tabulated by Blevins (1992). The important conclusion made visible in Figure 2 is that the optimal spacing increases when the screen becomes an increasingly more significant flow

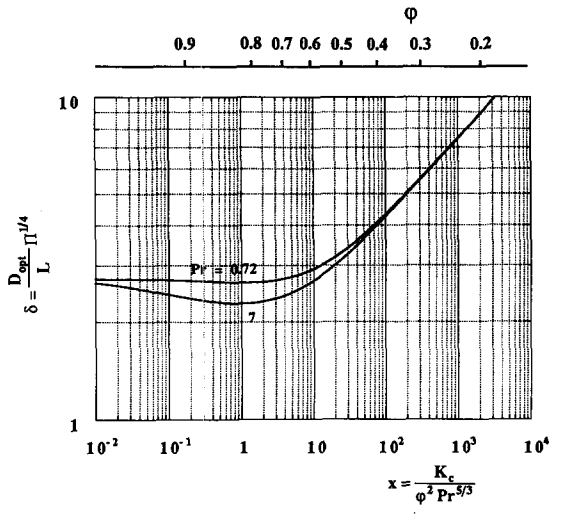

Figure 2 The optimal plate-to-plate spacing as a function of the screen characteristics when the stack is cooled by forced convection (high-screen Reynolds numbers). The upper φ scale refers to air cooling (Pr = 0.72) and screens made of plates with sharp-edged perforations

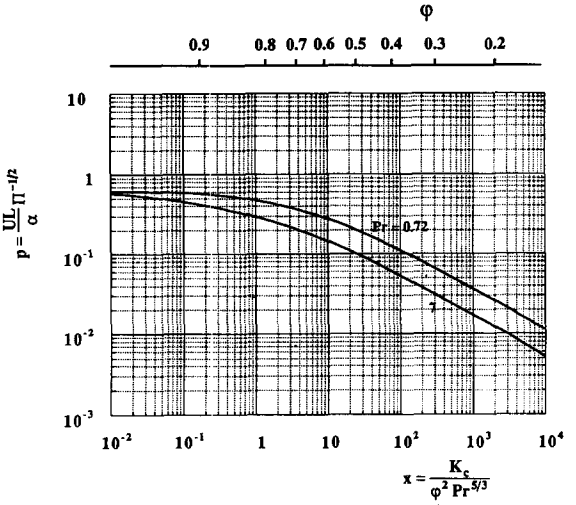

Figure 3 The screen effect on the flow through the stack during cooling by forced convection (high-screen Reynolds numbers). The upper φ scale refers to air cooling (Pr = 0.72) and screens made of plates with sharp-edged perforations

obstruction. The upper abscissa shows that the effect of the screens on the selection of D begins to be felt when the porosity φ drops below approximately 0.7. When screens with porosities greater than 0.7 are used, the optimal plate-to-plate spacing is the same as when the screens are absent.

Figure 3 shows the flow-rate solution $p(x)$, which accompanies the spacing solution $\delta(x)$ discussed until now. The p parameter is a modified Peclet number based on L and the mean velocity through the plate-to-plate channel, Equation 14. The figure shows that the flow rate decreases as x increases; i.e., as the screens become less permeable. In the case of air, the screen effect becomes important when x increases above approximately 1.

2.2 Stack with fixed plate-to-plate spacing

Another way of evaluating the effect of the screens on the thermal performance of the stack is by considering an existing stack (fixed D) that must be fitted with inlet and outlet screens. The new question is: how porous must the screens be so as not to decrease the thermal conductance between the stack and the coolant?

Let us assume that the existing stack has been optimized according to the design rule developed for stacks without screens, $\delta = 2.73$. Recall that the optimal design rests at the transition between the Hagen-Poiseuille regime, Equation 6, and the boundary-layer regime, Equation 10. When screens are added to the front and back of the stack and the overall ΔP remains unchanged, the flow-rate decreases, and the flow in each D-wide channel is definitely in the Hagen–Poiseuille regime. The screen–stack-screen assembly is described fully by Equations 6 and 7, which can be combined to eliminate U, and nondimensionalized by using Equations 13 with $\delta = 2.73$:

$$1.61[q'L/kH(T_w - T_\infty)\Pi^{1/2}] + (K_c/\varphi^2\ \mathrm{Pr})[q'L/kH(T_w - T_\infty)\Pi^{1/2}]^2 = 1 \qquad (17)$$

Equation 17 is plotted in Figure 4 to show the effect of the screens ($x_* = K_c/\varphi^2$ Pr) on the overall thermal conductance. It is clear that the screens have a detrimental effect, and this effect becomes sizeable when the new abscissa parameter x_* exceeds the range 1 – 10. In the case of air cooling, (Pr = 0.72) and screens with perforations with sharp edges (Blevins 1992), the screens induce a significant (greater than 20 percent) reduction in the overall thermal conductance if the porosity is smaller than 0.8. This critical porosity is comparable with the conclusion reached in the discussion of Figure 2. Note, further, that when φ is smaller than 0.8 in Figure 4, the overall thermal conductance decreases proportionally with φ.

2.3 Assembly cooled by a free stream

In the analysis presented above, we assumed that the pressure difference across the assembly is fixed, for example, by a fan situated downstream of the assembly. The same analysis is applicable to an assembly cooled by a free stream with the upstream velocity U_∞, Figure 1. Note that the pressure difference maintained by such a stream is approximately $\Delta P \cong (1/2)\rho U_\infty^2$. The results for such configurations are the

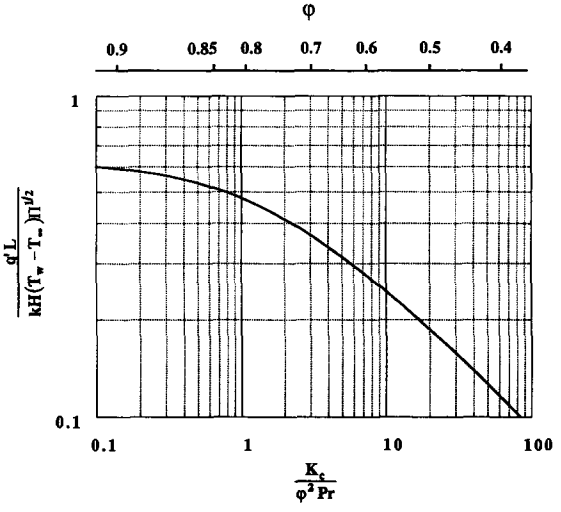

Figure 4 The effect of the screens on the overall thermal conductance when the plate-to-plate spacing D is fixed, and the cooling is by forced convection (high-screen Reynolds numbers). The upper φ scale refers to air cooling (Pr = 0.72) and screens made of plates with sharp-edged perforations

same as in Figures 2, 3, and 4, except that the pressure difference number Π, Equation 13, is replaced everywhere by the following group:

$$\Pi \cong (1/2)\ \mathrm{Pr}\ \mathrm{Re}_L^2 \tag{18}$$

where $\mathrm{Re}_L = U_\infty L/\nu$.

3. Forced convection: small screen Reynolds numbers

The results presented in Sections 2.1–2.3 are based on the assumption that the screen Reynolds number is large enough that the screen pressure drop is proportional to the velocity squared, Equation 3. The screen pressure drop behaves quite differently in the limit of small screen Reynolds numbers, where it is proportional to the velocity (Cornell 1958; Bernardi et al. 1976; Smetana 1963). In place of Equation 3, the total pressure drop is given by the following:

$$\Delta P = \Delta P_s + 2\lambda\, \mu\, U_\infty/d \tag{19}$$

where 2 is the number of screens, U_∞ is the approach velocity, d is the length scale of the screen (e.g., the wire diameter in a square-mesh screen), and $\lambda(\varphi)$ is a dimensionless coefficient depending only on screen porosity. Bernardi et al. showed that the following expression:

$$\lambda = 599 \exp(-7.01\ \varphi) \tag{20}$$

correlates within ± 5 percent pressure drop measurements with air and oil through square-mesh wire screens in the range $0.3 \le \varphi \le 0.61$, and $\mathrm{Re}_d < 10$, where $\mathrm{Re}_d = U_\infty d/\nu$ is the screen Reynolds number.

In Sections 3.1–3.3 we report only the results of the analysis analogous to Equations 1–18, in which the high-Re_d pressure drop model (Eq. 3) was replaced by the low-Re_d model presented in Equations 19 and 20. The numbering of Sec. 3.1–3.3 is intended to show the analogy with Sections 2.1–2.3, so that the omitted analytical steps can be retraced if needed.

3.1 The optimal plate-to-plate spacing

In place of Equations 15 and 16, the solution to the optimal spacing problem is obtained by solving the following system:

$$12p/\delta^2 + 2y = 1 \tag{21}$$

$$1.134\, y\, \delta^2 p^2\, \mathrm{Pr}^{1/3} + 0.567\, \delta^2 p^3 = 1 \tag{22}$$

where y is the new dimensionless screen parameter for the small Re_d limit:

$$y = \lambda(L/d)\Pi^{-1/2} \tag{23}$$

The solution is presented as $\delta(y)$ and $p(y)$ in Figure 5. The qualitative agreement between these curves and Figures 2 and 5 is clear. Just as x in Figures 2 and 3, the new screen parameter y increases when the screen porosity decreases. In the same direction, the optimal board-to-board spacing δ increases, and the velocity decreases. One new feature is that an optimal spacing exists only when the porosity is large enough that y is less than 0.5.

3.2 Stack with fixed plate-to-plate spacing

The effect of the screens on the total heat transfer rate is described by the following:

$$[q'L/k\, H(T_w - T_\infty)\Pi^{1/2}] = 1/(1.61 + 2y) \tag{24}$$

Here, we assumed that the spacing is fixed, having been selected

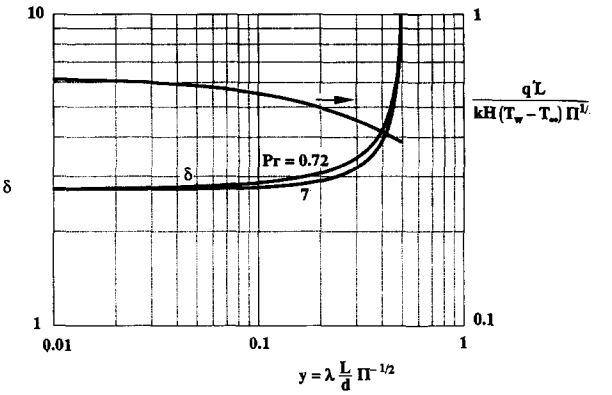

Figure 5 The effect of the screens on the optimal spacing and the flow when the cooling is by forced convection (low-screen Reynolds numbers). The right side shows the screen effect when the spacing is fixed

(optimized) when the screens were absent, $\delta = 2.73$. Equation 24 is plotted in Figure 5 and shows that the total heat transfer rate decreases as y increases; i.e., as the screen porosity decreases. The relation between y and porosity is illustrated by the numerical example given in the next section.

3.3 Assembly cooled by a free stream

As shown in Section 2.3, when the approach velocity U_∞ is specified (instead of ΔP), Equations 21–24 continue to hold, provided Π is replaced by $(1/2)\,\mathrm{Pr}\,\mathrm{Re}_L^2$, Equation 18. The screen parameter definition (Eq. 23) changes to the following:

$$y \cong (\lambda/\mathrm{Re}_d)(2/\mathrm{Pr})^{1/2} \tag{25}$$

For example, if $\mathrm{Re}_L = 1000$, $\mathrm{Pr} = 0.72$, $L = 10$ cm, and $d = 1$ mm, by using the correlation 20, we find that y covers the range between 120 and 14 when φ varies between 0.3 and 0.61 [as in Bernardi et al.'s (1976) correlation]. In this y range, the screens have a profound (detrimental) effect on the total heat transfer rate (cf. Equation 24).

4. Natural convection: large screen Reynolds numbers

We now turn our attention to a series of analogous questions for designs where the parallel plates are vertical, and the cooling is by natural convection. As shown in Figure 6, most of the modeling features described in connection with Figure 1 are repeated, with the difference that the swept length of each plate now is the height H. The assembly is immersed in a quiescent fluid of temperature T_∞. The number of parallel plates, $n = L/D$, is assumed to be considerably greater than 1.

To preserve the symmetry of the work and results presented so far, and to minimize the space used, we begin with the assumption that the screen Reynolds number is high enough that the screen pressure drop is described by the last term in Equation (3). The low Re_p regime is documented in Section 5, because it is likely to occur in small-size packages cooled by natural convection.

4.1 Optimal plate-to-plate spacing

We follow the analytical steps outlined in Section 2.1 and seek to determine the effect of the screen on the plate-to-plate

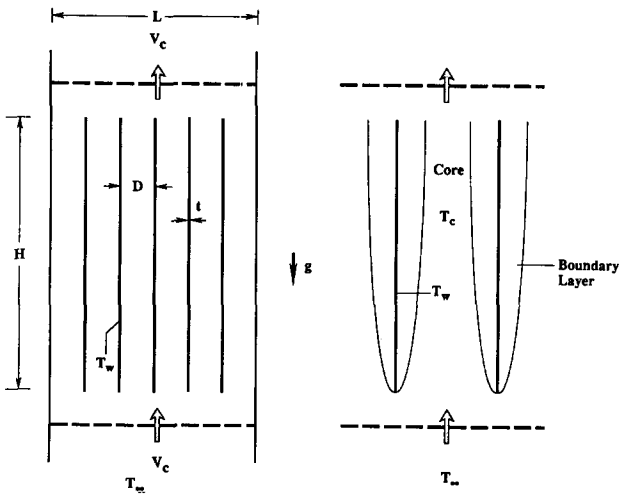

Figure 6 Natural convection cooling of a stack of parallel plates with inlet and outlet screens. Right side: distinct boundary layers and core temperatures in the large D limit

spacing D that maximizes the stack-ambient thermal conductance $q'/(T_w - T_\infty)$. The stack without inlet and outlet screens has been optimized already (Anand et al. 1990, 1992; Bar-Cohen and Rohsenow 1984; Bejan 1984; Elenbaas 1942; Kim et al. 1992; Levy 1971) and will be used as reference.

In the small D limit, the channels of width D contain fluid at a temperature approaching the plate temperature T_w. This means that the total pressure difference that drives the chimney flow is $\Delta P = \rho g H \beta (T_w - T_\infty)$; i.e., the difference between the hydrostatic pressures at the bottom of two H-tall columns, one filled with T_∞-fluid and the other with T_w-fluid. The driving pressure difference ΔP is opposed by two flow resistances in series, the Hagen–Poiseuille flow resistance of the parallel plates, and the pressure drop due to the screens:

$$\rho g H \beta (T_w - T_\infty) = 12\mu(HU/D^2) + 2K_c(1/2)\rho V_c^2 \tag{26}$$

where U is the mean velocity in the D channel. By using Equations 4 and 5, we rewrite Equation 18 as follows:

$$\rho g H \beta (T_w - T_\infty) = 12\mu(HU/D^2) + (K_c/\varphi^2)\rho U^2 \tag{27}$$

In the same small D limit, the total heat transfer from the stack to the chimney flow is as follows: (cf. Equation 7):

$$q'_{\text{small } D} = \rho U L c_p (T_w - T_\infty) \tag{28}$$

Consider next the large D limit where the vertical plates are lined by distinct boundary layers. The core of each D-wide channel is inhabited by fluid of temperature T_c, which generally is higher than the ambient temperature T_∞ because of the fluid trapping effect of the two screens. Only when the screens are absent does the core temperature T_c equal T_∞. With the screens in place, the pressure-driving effect is the difference between the hydrostatic pressures at the base of an H-tall column of T_∞-fluid and at the base of an adjacent H-tall column of T_c-fluid; namely, $\rho g H \beta (T_c - T_\infty)$. This driving effect is balanced entirely by the pressure drop across the screens:

$$\rho g H \beta (T_c - T_\infty) = 2K_c(1/2)\rho V_c^2 \tag{29}$$

The total heat transfer in the large D limit is $2n$ times the heat transfer through one boundary layer, $q'_1 = \bar{h} H (T_w - T_\infty)$ where $\bar{h} = \overline{Nu} k/H$, and $\overline{Nu} = 0.517[g\beta H^3(T_w - T_c)/\alpha\nu]^{1/4}$; e.g., Bejan (1993):

$$q'_{\text{large } D} = 1.034(L/D)k(T_w - T_c)[g\beta H^3(T_w - T_c)/\alpha\nu]^{1/4} \tag{30}$$

The analysis of the large D limit is completed by the first law argument that the heat transfer from the stack, Equation 30, must be balanced by the enthalpy picked up by the coolant as it rises through the assembly, $\dot{m}' c_p (T_c - T_\infty)$. The total mass flow rate through the stack is $\dot{m}' = \rho V_c \varphi L$, for which V_c is provided by Equation 29. In the end, this energy balance yields the following:

$$1.034(L/D)k(T_w - T_c)[g\beta H^3(T_w - T_c)/\alpha\nu]^{1/4} = \rho\varphi L c_p (T_c - T_\infty)[g\beta H(T_c - T_\infty)/K_c]^{1/2} \tag{31}$$

Finally, to locate the optimal plate-to-plate spacing that maximizes the thermal conductance $q'/(T_w - T_\infty)$ we set $q'_{\text{small } D} = q'_{\text{large } D}$ using Equations 28 and 30. The resulting relation is as follows:

$$UH/\alpha = 1.034\,(H/D_{\text{opt}})(1 - \theta)^{5/4}\,\text{Ra}_H^{1/4} \tag{32}$$

where

$$\theta = (T_c - T_\infty)/(T_w - T_\infty), \qquad \text{Ra}_H = g\beta H^3(T_w - T_\infty)/\alpha\nu \tag{33}$$

The dimensionless core temperature θ varies between 0 and 1.

To summarize, the natural convection problem reduces to solving Equations 27, 31, and 32 for three unknowns: D_{opt}, θ, and U. The numerical work of determining and displaying the solution is aided considerably by the use of the dimensionless groups:

$$\delta_* = (D_{\text{opt}}/H)\,\text{Ra}_H^{1/4}, \qquad x_* = K_c/\varphi^2\,\text{Pr}, \tag{34}$$

$$p_* = (UH/\alpha)\,\text{Ra}_H^{-1/2},$$

so that the optimal spacing is described by the constant $\delta_* = 2.32$ in the design without screens ($x_* = 0$). Equations 27, 31, and 32 become, respectively, as follows:

$$12p_*/\delta_*^2 + x_* p_*^2 = 1 \tag{35}$$

$$1.034(1 - \theta)^{5/4}/\theta^{3/2} = \delta_*/x_*^{1/2} \tag{36}$$

$$p_*\delta_* = 1.034(1 - \theta)^{5/4} \tag{37}$$

Figure 7 shows the $\delta_*(x_*)$ relation prescribed by Equations 35–37. The optimal spacing decreases as the abscissa parameter increases; i.e., as the screens pose an increasing flow resistance. The decrease in δ_* *vs.* x_* is interesting because it runs against the trend exhibited by the corresponding result for forced convection [see the curve $\delta(x)$ in Figure 2]. Interesting also are the similarities between Figures 7 and 2, specifically, the nearly

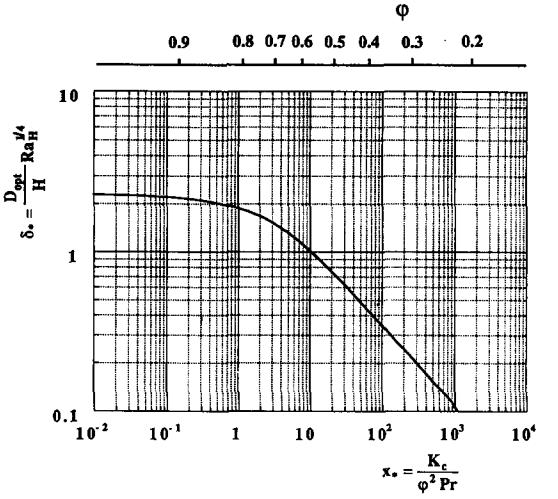

Figure 7 The optimal plate-to-plate spacing as a function of the screen characteristics when the stack is cooled by natural convection (high-screen Reynolds numbers). The upper φ scale refers to air cooling (Pr = 0.72) and screens made of plates with sharp-edged perforations

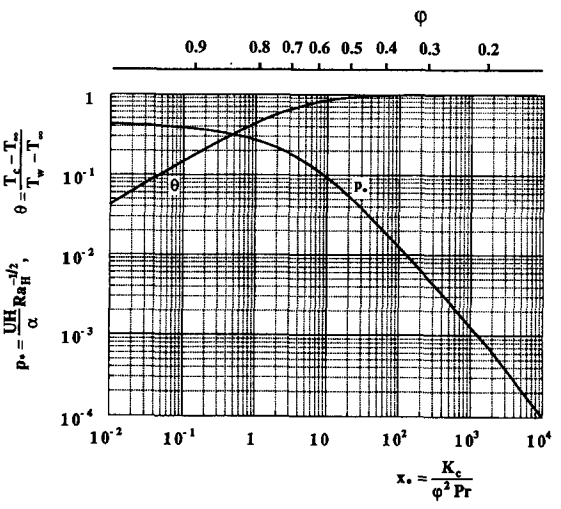

Figure 8 The screen effect on the flow through the stack and the core temperature during cooling by natural convection (high-screen Reynolds numbers). The upper φ scale refers to air cooling (Pr = 0.72) and screens made of plates with sharp-edged perforations

the same abscissa parameters, and the fact that the effect of the screens becomes important when the abscissa parameter exceeds a critical order of magnitude. In Figure 7, the knee of the $\delta_*(x_*)$ curve is located in the vicinity of $x_* \sim 1$, which in the case of air cooling and plate screens with sharp-edged perforations, means that the screen effect becomes important when the porosity falls below approximately 0.8.

Equations 35–37 also yield the functions $p_*(x_*)$ and $\theta(x_*)$, which are displayed in Figure 8. The modified Peclet number p_* decreases as x_* increases, which means that the flow slows as the screen porosity decreases. The dimensionless core temperature θ approaches 1 as x_* increases. This trend is expected, because the channel fluid becomes trapped as the screen openings close, and, as a result, the core temperature T_c approaches the plate temperature T_w.

4.2 Stack with fixed plate-to-plate spacing

Now consider the design in which the stack is given (D is fixed), and the screen porosity must be chosen so that the stack-ambient thermal conductance does not deteriorate. As in Section 2.2, we assume that the given stack spacing has been optimized based upon the rule valid for stacks without screens, namely $\delta_* = 2.32$ or $D = 2.32\, H\, \mathrm{Ra}_H^{-1/4}$. Without screens, the flow in each D-wide channel is at the transition between Hagen–Poiseuille flow and boundary layer flow.

When screens are fitted to the bottom and top of the stack, the flow rate is smaller than when the screens are absent, and the flow in each parallel plate channel is definitely of the Hagen–Poiseuille type. The thermal performance of the stack is described by Equations 27 and 28, which can be combined by eliminating U:

$$2.23q'H/kL(T_w - T_\infty)\mathrm{Ra}_H^{1/2} + (K_c/\varphi^2\ \mathrm{Pr})[q'H/kL(T_w - T_\infty)\mathrm{Ra}_H^{1/2}]^2 = 1 \qquad (38)$$

This equation describes the general effect of the screen ($x_* = K_c/\varphi^2\ \mathrm{Pr}$) on the overall thermal conductance; the latter has been nondimensionalized as the group shown inside the second set of square brackets. Equation 38 has the same form as Equation 17: this means that, graphically, Equation 38 will look almost the same as the curve shown in Figure 4, except that the new group on the ordinate will be $q'H/kL(T_w - T_\infty)\mathrm{Ra}_H^{1/2}$.

In conclusion, the effect of the horizontal screens is to decrease the stack-ambient thermal conductance as the screen porosity decreases below a critical order of magnitude. As indicated in the discussion of Figure 4, when the coolant is air, and the perforated plates have porosities smaller than approximately 0.8, installation of two screens induces a significant decrease in the overall thermal conductance of the package.

5. Natural convection: small screen Reynolds numbers

5.1 Optimal plate-to-plate spacing

The screen pressure drop behaves as shown in the second term on the right side of Equation 19. To obtain optimal plate-to-plate spacing, we repeated the analysis shown in Section 4.1, by starting with the following:

$$\rho g H \beta (T_w - T_\infty) = 12\mu\,(HU/D^2) + 2\lambda\mu U/d \qquad (39)$$

in place of Equation 26. The problem reduces to solving the following system:

$$12(p_*/\delta_*^2) + 2y_* p_* = 1 \qquad (40)$$

$$1.034(1-\theta)^{5/4}/\theta^2 = \delta_*/2y_* \qquad (41)$$

$$p_*\delta_* = 1.034(1-\theta)^{5/4} \qquad (42)$$

where δ_* and p_* are defined by Equations 34, and y_* is the new, dimensionless screen parameter

$$y_* = \lambda(H/d)\ \mathrm{Ra}_H^{-1/2} \qquad (43)$$

The results for the optimal spacing $\delta_*(y_*)$, velocity $p_*(y_*)$, and core temperature $\theta(y_*)$ are presented in Figure 9. The trends of these curves are the same as those in Figures 6 and 7 for higher-screen Reynolds numbers. The main difference is the definition of the dimensionless screen parameter; namely, y_* of Equation 43 in place of x_* of Equation 34.

5.2 Stack with fixed plate-to-plate spacing

The effect of adding screens to a vertical stack with optimized and fixed spacing is described by the following:

$$[q'H/kL(T_w - T_\infty)\mathrm{Ra}_H^{1/2}] = 1/(0.97 + 2y_*) \qquad (44)$$

The total heat transfer rate is sensitive to changes in the screen parameter. Consider the following numerical example.

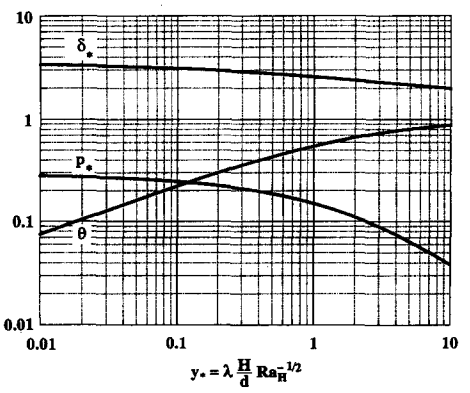

Figure 9 The effect of the screens as the optimal spacing, flow, and core temperature during cooling by natural convection (low-screen Reynolds numbers)

A vertical stack with $H = 10$ cm, $d = 1$ mm, and $(T_w - T_\infty) \sim 75$K in air is characterized by $Ra_H \sim 5 \times 10^6$. According to Equations 20 and 43, y_* covers the range $0.4 - 3.3$ as φ decreases from 0.61 to 0.3. Equation 44 shows that, in this range, the total heat transfer rate drops to between 1/2 and 1/10 of its value when the screens are absent.

6. Concluding remarks

In this paper, we considered the fundamental heat transfer problem of how to cool a stack of heat-generating boards that are surrounded by electromagnetic screens. We pursued this question by solving four distinct problems, which are all new:

(1) forced convection and screened stack with board-to-board spacing that must be selected to minimize the overall thermal resistance between stack and coolant;
(2) forced convection and screened stack with fixed board-to-board spacing;
(3) natural convection and vertical screened stack with board-to-board spacing that must be selected to minimize the overall thermal resistance; and
(4) natural convection and vertical screened stack with fixed board-to-board spacing.

The recommendations made for designs 1 and 2 have been extended to designs where the screened stack is cooled by immersion in a free stream (Section 2.3). We show that it is possible to condense the description of the effect of the screen characteristics by using the following dimensionless groups: x for forced convection at high Re_p; x_* for forced convection at low Re_p; y for natural convection at high Re_p; and y_* for natural convection at low Re_p. This description is very powerful because it makes the present results applicable to screens of several geometries, each geometry being characterized by its own $K_c(\varphi)$ or $\lambda(\varphi)$ function. Numerical examples show how the present results can be used in applications with air cooling and screens made of plates with sharp-edged perforations, and wire meshes.

We end with two observations about the method employed in this study. First, in the analytical method of intersecting the asymptotic solutions for small D and large D (Sections 2.1, 3.1, 4.1, and 5.1), we treated each plate as isothermal at the temperature T_w. For stacks of printed circuit boards, a more appropriate boundary condition is uniform heat flux, or distributed heat flux (discrete heat sources). The isothermal plate model is very good, for the purpose of determining the optimal spacing accurately. Bejan and Sciubba (1992) used an accurate analysis to demonstrate that the switch from constant temperature to constant flux surface conditions has practically no effect on the optimal spacing. Morega and Bejan (1994) performed complete numerical simulations of packages with discrete (flush mounted and protruding) heat sources and found that the optimal spacing determined numerically is anticipated very well by the intersection of asymptotes method.

Second, we chose to conduct this study analytically because the intersection of asymptotes method has been tested extensively. The empirical porous screen information collected from handbooks is also highly reliable: it is used routinely for design purposes in the electronic cooling industry. In natural convection, there is excellent agreement between the intersection of asymptotes results (Bejan, 1984), and accurate analytical results (Bar-Cohen and Rohsenow, 1984) and the results of complete numerical simulations (Anand, et al., 1990, 1992). In forced convection, the excellent agreement between the intersection of asymptotes method and accurate analysis of entrance-type flow (of the type used by Bar-Cohen and Rohsenow 1984) was documented by Bejan and Sciubba (1992). On the experimental side, Morega et al. (1995) found excellent agreement between the results of the intersection of asymptotes method and the optimal spacings determined experimentally by Hirata et al. (1970), Nakayama et al. (1988) and Matsushima et al. (1992).

The present study was one of thermal design optimization, where we used tested methods for the purpose of generating fundamental results for several classes of thermal design problems. Indeed, one contribution of this study was to introduce the *intersection of asymptotes method* to thermal designers who otherwise might conduct extensive (and expensive) numerical simulations of the flow and heat transfer in large numbers of different package geometries.

Acknowledgment

This work was sponsored by the IBM Corporation, Research Triangle Park, North Carolina. Dr. Alex J. Fowler's assistance is appreciated very much.

References

Anand, N. K., Kim, S. H. and Fletcher, L. S. 1990. The effect of plate spacing on free convection between heated parallel plates. *ASME HTD*, **153**, 515–518

Anand, N. K., Kim, S. H. and Fletcher, L. S. 1992. The effect of plate spacing on free convection between heated parallel plates. *J. Heat Transfer*, **114**, 515–518

Bar-Cohen, A. and Rohsenow, W. M. 1984. Thermally optimum spacing of vertical, natural convection cooled, parallel plates. *J. Heat Transfer*, **106**, 116–123

Bejan, A. 1984. *Convection Heat Transfer*, Wiley, New York, p. 157, Problem 11

Bejan, A. 1993. *Heat Transfer*, Wiley, New York, 331–332

Bejan, A. and Sciubba, E. 1992. The optimal spacing of parallel plates cooled by forced convection. *Int. J. Heat Mass Transfer*, **35**, 3259–3264

Bernardi, R. T., Linehan, J. H. and Hamilton, L. H. 1976. Low Reynolds number loss coefficient for fine mesh screens. *J. Fluids Eng.*, **98**, 762–764

Blevins, R. D. 1992. *Applied Fluid Dynamics Handbook*, Krieger, Malabar, FL, 314

Cornell, W. G. 1958. Losses in flow normal to plane screens. *ASME Trans.*, **80**, 791–799

Elenbaas, W. 1942. Heat dissipation of parallel plates by free convection. *Physica*, **9**, 1–23

Ellison, G. N. 1984. *Thermal Computations for Electronic Equipment*, Van Nostrand Reinhold, New York, chap. 6

Hirata, M., Kakita, Y., Yada, Y., Hirose, Y., Morikawa, T. and Enomoto, H. 1970. Temperature distribution of finned integrated circuits. *Fujitsu Sci. & Tech. J.*, **6**, 91–115

Idelchik, I. E., Malyavskaya, G. R., Martynenko, O. G. and Fried, E. 1986. *Handbook of Hydraulic Resistance*, 2nd ed., Hemisphere, Washington, DC, 408

Incropera, F. P. and DeWitt, D. P. 1990. *Fundamentals of Heat and Mass Transfer*, Wiley, New York

Kim, S. H., Anand, N. K. and Fletcher, L. S. 1991. Free convection between series of vertical parallel plates with embedded line heat sources. *J. Heat Transfer*, **113**, 108–115

Levy, E. K. 1971. Optimum plate spacing for laminar natural convection heat transfer from parallel vertical isothermal flat plates. *J. Heat Transfer*, **93**, 463–465

Matsushima, H., Yanagida, T. and Kondo, Y. 1992. Algorithm for predicting the thermal resistance of finned LSI packages mounted on a circuit board. *Heat Transfer Japanese Res.*, **21**, 504–517

Mereu, S., Sciubba, E. and Bejan, A. 1993. The optimal cooling of a stack of heat generating boards with fixed pressure drop, flowrate or pumping power. *Int. J. Heat Mass Transfer*, **36**, 3677–3686

Morega, A. M. and Bejan, A. 1994. Optimal spacing of parallel boards with discrete heat sources cooled by laminar forced convection. *Num. Heat Transfer, Part A*, **25**, 373–392

Morega, A. M., Bejan, A. and Lee, S. W. 1995. The optimal cooling of a stack of parallel plates in a free stream. *Int. J. Heat Mass Transfer*, **38**, to appear

Nakayama, W., Matsushima, H. and Goel, P. 1988. Forced convective heat transfer from arrays of finned packages. *Cooling Technology for Electronic Equipment*, W. Aung (ed.). Hemisphere, New York, 195–210

Ott, H. W. 1988. *Noise Reduction Techniques in Electronic Systems*, 2nd ed., Wiley, New York, chap. 6

Smetana, F. O. 1963. On the prediction of gas flow rates through round wire screens. *J. Basic Eng.*, **85**, 620–624

Steinberg, D. S. 1980. *Cooling Techniques for Electronic Equipment*, Wiley, New York, chap. 8